

Gravitational Collapse with a Cosmological Constant

Dragoljub Markovic¹ and Stuart L. Shapiro^{1,2}

¹ *Department of Physics, University of Illinois at Urbana-Champaign, Urbana, IL 61801*

² *Department of Astronomy and NCSA, University of Illinois at Urbana-Champaign, Urbana, IL 61801*
(August 8, 2018)

We consider the effect of a positive cosmological constant on spherical gravitational collapse to a black hole for a few simple, analytic cases. We construct the complete Oppenheimer-Snyder-deSitter (OSdS) spacetime, the generalization of the Oppenheimer-Snyder solution for collapse from rest of a homogeneous dust ball in an exterior vacuum. In OSdS collapse, the cosmological constant may affect the onset of collapse and decelerate the implosion initially, but it plays a diminishing role as the collapse proceeds. We also construct spacetimes in which a collapsing dust ball can bounce, or hover in unstable equilibrium, due to the repulsive force of the cosmological constant. We explore the causal structure of the different spacetimes and identify any cosmological and black hole event horizons which may be present.

PACS numbers: 95.30.Sf, 98.80.Hw, 04.20.Jb

I. INTRODUCTION

Recent measurements of Type Ia supernovae suggest that our universe may have a nonzero cosmological constant $\Lambda > 0$ [1,2]. A more recent analysis [3] of the peculiar motion of low-redshift galaxies seems to give further evidence for a finite Λ . Obviously, such an interpretation of the data, if correct, will have huge implications for cosmology. More generally, if a cosmological constant must be restored to Einstein's equations of general relativity, surprises may turn up in other physical applications of Einstein's field equations, although the small size of the constant precludes its having a significant effect on the scale of typical galaxies, stars or planets. It is therefore interesting to consider, at least as a point of principle, what impact, if any, the presence of a finite cosmological constant has on our conventional picture of gravitational collapse to a black hole. Many of the important dynamical and geometric features of catastrophic collapse in the absence of a cosmological constant are revealed by the analytic Oppenheimer-Snyder model [4], which describes the collapse of a spherical, homogeneous dust ball, initially at rest in an exterior vacuum, to a Schwarzschild black hole. In this paper we generalize this model accounting for the presence of a positive cosmological constant. We also consider closely related, dust ball solutions for which the implosion does not begin at rest.

There are a number of questions that motivate our analysis: How does the cosmological constant, which acts as a repulsive force, affect the motion and fate of a collapsing object? Under what circumstances, if any, can a cosmological constant *prevent* the collapse of a dust ball which is initially imploding? What is the global horizon structure of an exponentially expanding universe containing a collapsing dust ball? When do black holes form?

II. DYNAMICS OF A HOMOGENEOUS DUST SPHERE WITH COSMOLOGICAL CONSTANT

The interior of a homogeneous sphere is given by the Friedmann-Robertson-Walker (FRW) metric

$$ds^2 = -d\tau^2 + a^2 \left[\frac{dx^2}{1 - kx^2} + x^2 (d\theta^2 + \sin^2 \theta d\phi^2) \right], \quad (2.1)$$

where $k = -1, 0$ or 1 for a hyperbolic, flat or spherical spatial geometry, respectively. The density remains homogeneous on spatial slices of constant time τ . The surface of the sphere is located at constant $x = X$, where $0 \leq X < 1$. Einstein's equations for a pressureless fluid (i.e., "dust") of density μ/a^3 in the presence of cosmological constant Λ yield

$$\left(\frac{\dot{a}}{a} \right)^2 = \frac{8\pi}{3} \frac{\mu}{a^3} - \frac{k}{a^2} + \frac{\Lambda}{3}. \quad (2.2)$$

This interior spacetime is often called the Friedmann-Lemaître (FL) universe.

The standard Oppenheimer-Snyder (OS) solution [4] for the interior of a collapsing homogeneous dust sphere, initially at rest, is a piece of a closed FL ($k = 1$) universe with $\Lambda = 0$. In OS collapse, the initial time-slice $\tau = 0$ is defined at the moment of time-symmetry at maximum expansion, when the right hand side of Eq. (2.2) vanishes. The same form for the interior metric with $k = 1$ applies in the presence of a cosmological constant. The solution we seek – collapse of a spherical dust ball from rest in an exponentially expanding universe with a positive cosmological constant – we shall refer to as an Oppenheimer-Snyder-de Sitter (OSdS) spacetime.

According to the generalized Birkhoff theorem [5], the vacuum spacetime outside the sphere is Schwarzschild-de Sitter (SdS) [6]

$$ds^2 = -f dt^2 + \frac{1}{f} dr^2 + r^2 (d\theta^2 + \sin^2 \theta d\phi^2),$$

$$f(r) = 1 - \frac{2M}{r} - \frac{\Lambda}{3} r^2 \quad (2.3)$$

where M is a constant. This spacetime represents the vacuum exterior of a spherical mass immersed in the exponentially expanding (at large r) de Sitter space.

We neglect for the moment the presence of the dust sphere and assume that metric (2.3) describes the entire spacetime with r in the range $0 < r < \infty$. The metric function $f(r)$ (see Fig. 1) reaches the maximum value $f_{\max} = 1 - (9M^2\Lambda)^{1/3}$ at $r_m = (3M/\Lambda)^{1/3}$. Thus, for $M < 1/3\Lambda^{1/2}$, $f(r)$ has two real positive roots, r_h and $r_c > r_h$, where

$$r_{h,c} = \frac{2}{\Lambda^{1/2}} \sin \left[\frac{1}{3} \sin^{-1} \left(3M\Lambda^{1/2} \right) + n \frac{2\pi}{3} \right]$$

$$n = 0, 1 \quad (2.4)$$

(we choose $0 \leq \sin^{-1} A \leq \pi/2$ for $0 \leq A \leq 1$; the third root is negative, $r_3 = -r_h - r_c$). For all null and timelike geodesics crossing the *black hole horizon* $r = r_h$ inward, $-\partial_r$ is the future-directed timelike vector, and so they all terminate at the singularity $r = 0$. All the future and outward-directed (timelike or null) geodesics at $r > r_h$ cross the *cosmological horizon* $r = r_c$ and ultimately reach cosmological null infinity I^+ at late times.

Returning now to the motion of a dust sphere with the exterior spacetime (2.3), we match the spacetime geometry across the sphere's surface $r = R(\tau)$ ($x = X = \text{const}$) which requires (1) the continuity of the surface's 3-metric

$$^{(3)}ds^2 = -d\tau^2 + R^2 (d\theta^2 + \sin^2 \theta d\phi^2), \quad (2.5)$$

where $R(\tau) = Xa(\tau)$, as well as (2) the junction condition $[K_j^i] \equiv K_j^i|_{\text{out}} - K_j^i|_{\text{in}} = 0$, for the extrinsic curvature [7]

$$K_{ij} \equiv -\mathbf{e}_i \cdot (\nabla_j \mathbf{n}) = \mathbf{n} \cdot (\nabla_j \mathbf{e}_i). \quad (2.6)$$

The three vectors \mathbf{e}_i are intrinsic to the spacetime hypersurface swept by the moving surface, $\mathbf{u} = \dot{t}\partial_t + \dot{R}\partial_r$ ($\dot{t} \equiv dt/d\tau$), ∂_θ and ∂_ϕ , while $\mathbf{n} = n^t\partial_t + n^r\partial_r$ is the outward-directed unit 4-vector orthogonal to the surface. From the orthonormality conditions

$$-1 = \mathbf{u} \cdot \mathbf{u} = -\dot{t}^2 + \frac{1}{f} \dot{R}^2,$$

$$0 = \mathbf{u} \cdot \mathbf{n} = -\dot{t}n^t + \frac{1}{f} \dot{R}n^r,$$

$$1 = \mathbf{n} \cdot \mathbf{n} = -f(n^t)^2 + \frac{1}{f} (n^r)^2, \quad (2.7)$$

and the metric forms (2.1) and (2.3), we obtain the t -component of the 4-velocity

$$\dot{t} = \eta_1 \frac{(\dot{R}^2 + f)^{1/2}}{|f|}, \quad \eta_1 = \pm 1, \quad (2.8)$$

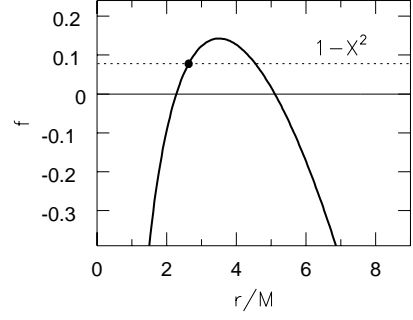


FIG. 1. The effective potential $f(r)$ ($\Lambda = 0.07/M^2$, $X = 0.96$). Oppenheimer-Snyder-de Sitter (OSdS) collapse starts from rest at the dot and proceeds inward (leftward along the dotted line).

and components of the unit normal

$$n^r = \eta_2 \left(f + \dot{R}^2 \right)^{1/2}, \quad n^t = \frac{\eta_2 \dot{R}}{\eta_1 |f|}, \quad (2.9)$$

($\eta_2 = \pm 1$) on the outside, and

$$n^r = 0, \quad n^x = \frac{\sqrt{1 - kX^2}}{a}, \quad (2.10)$$

on the inside of the surface.

The condition $[K_\theta^\theta] = 0$, where

$$K_{\theta\theta}|_{\text{out}} = \mathbf{n} \cdot \Gamma_{\theta\theta}^i \mathbf{e}_i = -\frac{1}{2} n^r g_{\theta\theta,r}|_{r=R} = -Rn^r,$$

$$K_\theta^\theta|_{\text{out}} = -\frac{n^r}{R},$$

$$K_{\theta\theta}|_{\text{in}} = n^x \Gamma_{x\theta\theta} = -\frac{1}{2} n^x g_{\theta\theta,x}|_{x=X} = -n^x a^2 X,$$

$$K_\theta^\theta|_{\text{in}} = -\frac{n^x}{X}, \quad (2.11)$$

implies $\eta_2 = 1$ and leads to the equation that describes motion in the effective potential $f(R)$ (see Fig. 1)

$$\dot{R}^2 + f(R) = 1 - kX^2. \quad (2.12)$$

Comparing Eqs. (2.2) and (2.12) we identify

$$M = \frac{4\pi}{3} \mu X^3. \quad (2.13)$$

(The junction conditions for other components of the extrinsic curvature do not yield additional information.)

For $k = 1$ there is a range of parameters, $M \leq 1/3\Lambda^{1/2}$ and $X > (9M^2\Lambda)^{1/6}$, for which equation $0 = 1 - X^2 - f = \Lambda r^2/3 + 2M/r - X^2$ has three real roots, out of which two, r_o and $r_b > r_o$ are positive

$$r_{o,b} = \frac{2X}{\Lambda^{1/2}} \sin \left[\frac{1}{3} \sin^{-1} \left(3M\Lambda^{1/2}/X^3 \right) + n \frac{2\pi}{3} \right]$$

$$n = 0, 1. \quad (2.14)$$

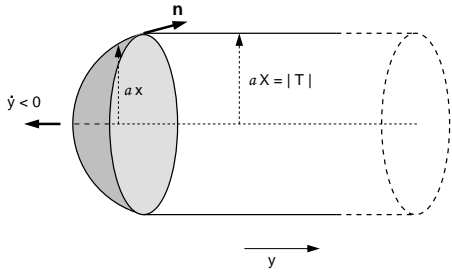


FIG. 2. A dust ball with an exterior whose spacelike hypersurfaces have cylindrical geometry [see Eq. (2.15)]. One angular dimension is suppressed. The dust ball recedes leftward ($\dot{y} < 0$) as viewed from the exterior. The interface ($x = X$) normal \mathbf{n} is drawn tangential to the sphere's interior.

The third root, $\bar{r}_3 = -r_b - r_o$ is then negative. According to Eq. (2.12), the sphere at $R = r_o$ or $R = r_b$ is momentarily at rest.

For $f(r) > 0$ [8], t is a timelike future-directed coordinate and Eq. (2.8) implies $\eta_1 = 1$. If, on the other hand, $r < r_h$ or $r > r_c$, so that $f(r) < 0$ [assuming $f(r)$ has positive roots], r is timelike. If, in addition, $-\partial_r$ is future-directed [9], it is convenient to introduce the new notation, $T \equiv -r < 0$ and $y \equiv t$, in which metric (2.3) takes on the time-dependent form

$$ds^2 = -\frac{1}{g}dT^2 + gdy^2 + T^2(d\theta^2 + \sin^2\theta d\phi^2),$$

$$g(T) = \frac{\Lambda}{3}T^2 - \frac{2M}{T} - 1 > 0. \quad (2.15)$$

Metric (2.15) describes a 3-dimensional cylindrical space-like hypersurface of radius $|T|$, symmetric around its y -axis (see Fig. 2). For $r < r_h$, this hypersurface contracts radially and expands in the y -direction from zero size at the coordinate singularity $T = -r_h$, to an infinite extent at the physical singularity $T = 0$. For $r_c < r < \infty$, it contracts in the radial direction and along its y -axis until the coordinate singularity $g(T) = 0$ is reached at time $T = -r_c$.

The vacuum spacetime given by metric (2.15) may extend to infinity in both directions along the y -axis. Alternatively, it can be bounded on the left (so that \mathbf{n} points toward increasing y , $n^y = n^t > 0$; see Fig. 2) by the surface of an inevitably contracting sphere [$\dot{R} = -\dot{T} < 0$, and thus $\eta_1 = -1$; see Eq. (2.9)] that recedes leftward,

$$\dot{y} = -\frac{\sqrt{1 - kX^2}}{g}, \quad (2.16)$$

along the y axis. The trajectory of the surface is given by

$$\frac{dy}{dT} = -\frac{\sqrt{1 - kX^2}}{g\sqrt{1 - kX^2 + g}}$$

$$\approx \begin{cases} -\left(\frac{3}{\Lambda}\right)^{3/2} \frac{\sqrt{1 - kX^2}}{T^3} & (\text{for } T \rightarrow -\infty) \\ -\sqrt{1 - kX^2} \left(\frac{T}{2M}\right)^{3/2} & (\text{for } T \rightarrow 0). \end{cases} \quad (2.17)$$

For $r < r_h$, the sphere's surface therefore starts at $T = -r_h$, where $g \propto T - T_h \rightarrow 0$, at which point $\dot{y} \rightarrow -\infty$ and $y \rightarrow \infty$, and reaches some finite $y = y_f$ at $T = 0$. For $r > r_c$, the surface travels from a finite $y = y_i$, at $T = -\infty$, to $y = -\infty$ at $T = -r_c$.

If, on the other hand, we place the contracting sphere to the right of the vacuum sector given by metric (2.15), $n^y < 0$ (and thus $\eta_1 = 1$), and the sphere's surface will recede toward increasing y , $\dot{y} > 0$. If r is a future-directed timelike coordinate [10] (so that the notation change would be $T \equiv r$, $y \equiv t$), the motion of the sphere is reversed: it expands, $\dot{R} = \dot{T} > 0$ and, if, e.g., placed on the left, $n^y > 0$, it advances to the right, $\dot{y} > 0$.

III. BOUNCING SPHERE

As discussed in the previous section, for $k = 1$ we have the range of parameters, $M \leq 1/3\Lambda^{1/2}$ and $X > (9M^2\Lambda)^{1/6}$, for which a dust sphere contracting from large radii will bounce at $R = r_b > r_h$, where r_b is the larger of the two positive roots of the equation $f(r) = 1 - X^2$ (see Fig. 1).

The Penrose diagram for the complete spacetime is given in Fig. 3. At large negative time τ (between the past null infinity I^- and the past cosmological horizon \mathcal{H}_c^-) the dynamics is dominated by the cosmological constant and the sphere contracts exponentially, $R \propto \exp(-\sqrt{\Lambda/3}\tau)$. After the sphere's surface has crossed \mathcal{H}_c^- , it will reverse its motion at $R = Xa(\tau = 0) = r_b$ and then expand toward the future cosmological horizon \mathcal{H}_c^+ , and ultimately the future null infinity I^+ . In contrast to an implosion in a static Schwarzschild background, the presence of a positive cosmological constant is sufficient to halt and reverse the collapse in this case. Here the presence of the dust does not alter in essence the familiar bounce of the spherical spatial hypersurfaces near the ‘‘throat’’ of the de Sitter spacetime [11].

The presence of a massive sphere, however, is not entirely without an effect on the global structure of the spacetime. In the limit of vanishing mass M , the radial null ray that enters the sphere at the exact moment when its surface crosses the future cosmological horizon (\mathcal{H}_c^+) radius, $R = r_c$, will take an infinite time τ to reach the re-expanding sphere's center $x = 0$. On the other hand (see the Appendix), for any finite mass $M > 0$, the null ray will reach the center in a finite time, then proceed outward and reach some finite $x = x_f$ at infinitely late times. In this case, the surface r_c no longer has the significance of a cosmological horizon [12] with respect to an observer at $x = 0$.

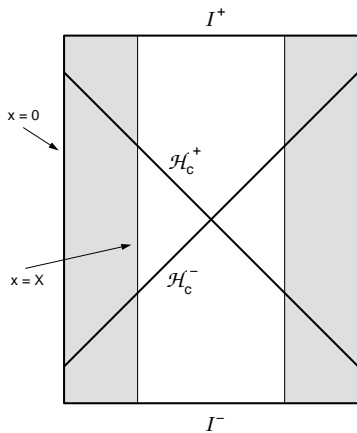


FIG. 3. The Penrose diagram for the spacetime containing a “bouncing” dust sphere. The bouncing dust sphere to the right (identical to the one on the left side) is introduced for geodesic completeness.

The spacetime shown in Fig. 3 is geodesically complete, i.e., all geodesics extend to infinite values of their affine parameters in both directions. To achieve the completeness we have placed another dust sphere at the right of Fig. 2 and Fig. 3. While the second sphere must have the same values of M and Λ , we are free to choose for it any values of k_r and X_r , independent of the choices k and X for the sphere at the left. Of the great variety of combinations of two dust spheres, we will in this paper discuss only a few. The choice we have made in Fig. 3 is symmetric, i.e, $k_r = k = 1$ and $X_r = X$. Since the centers of the spheres cross the null rays \mathcal{H}_c^+ or \mathcal{H}_c^- , the two spheres are in causal contact. [Other ways of extending the spacetime to the right — with either massive spheres or interiors of black holes — are discussed in the next section.]

IV. COLLAPSING SPHERE

For the range of parameters discussed in the previous section, $M \leq 1/3\Lambda^{1/2}$ and $X > (9M^2\Lambda)^{1/6}$, one can follow the motion of the sphere at $R < R_i$, where R_i is smaller of the two positive roots of the equation $f(r) = 1 - X^2$. The sphere’s surface springs out of the past singularity at $r = 0$ (see Fig. 4), then emerges through the past black hole horizon \mathcal{H}_h^- , reverses its expansion at $R = R_i$, plunges through the future black hole horizon \mathcal{H}_h^+ , and finally ends in the future singularity at $r = 0$. As discussed in Section 2, the spacetime exterior to the sphere, usually called the Schwarzschild-de Sitter (SdS) spacetime [6], is characterized by two pairs of horizons: the future and past black hole horizons at $r = r_h$, and the future \mathcal{H}_c^+ and past \mathcal{H}_c^- cosmological horizon at $r = r_c$.

In this scenario the sphere always stays inside the cosmological horizon at r_c . If we follow the sphere’s implosion from the moment of time-symmetry at maximum

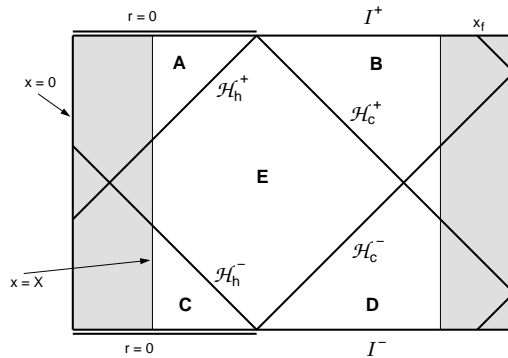


FIG. 4. Collapse to a black hole in the Schwarzschild-de Sitter universe. The dust sphere’s surface emerges from the past singularity through the past black-hole horizon, stops its expansion at point Ψ and then recollapses to a black hole. The Oppenheimer-Snyder-de Sitter (OSdS) collapse to a black hole starts from the moment of time-symmetry. The bouncing sphere, $X_r > (9M^2\Lambda)^{1/2}$, of mass M on the right side is introduced for geodesic completeness; it can be replaced by another re-collapsing sphere. The black-hole horizon structure corresponds to region **II** in the parameter space of Fig. 6.

expansion $R = r_o$ (Ψ in Fig. 4), the motion is a straightforward generalization for a non-vanishing cosmological constant Λ of the familiar Oppenheimer-Snyder collapse. The collapse is homologous and the density remains homogeneous on $\tau = \text{constant}$ time slices. Qualitatively, the cosmological constant serves as a perturbation whose influence on the collapse diminishes as the collapse progresses. We illustrate the initial braking effect of Λ on the collapse in Fig. 5 for the indicated values of ΛM^2 . We measure the sphere’s time in the units of the proper time, $T_{\Lambda=0} = \pi (R_i^3/8M)^{1/2}$, that a sphere would take to evolve from the static point at $R = R_i$ all the way to the final singularity in the case of a *vanishing* Λ .

In the left portion of Fig. 4, the past black hole horizon \mathcal{H}_h^- reaches the center of the sphere $x = 0$ after the future black hole horizon \mathcal{H}_h^+ has emerged from the origin. This configuration of the black-hole horizons would, e.g., make it impossible for an observer at $x = 0$ to take off in the radial direction and escape from the black hole after receiving the earliest possible signal from the past null infinity I^- . As we discuss in the Appendix, this is the case for the sector **II** in the plane of parameters X and $(9\Lambda M^2)^{1/6}$ shown in Fig. 6.

For the values of the parameters from sector **I** of Fig. 6, on the other hand, the arrival of \mathcal{H}_h^- at $x = 0$ precedes the departure of \mathcal{H}_h^+ . This case is shown in Fig. 7.

For any values of M and Λ (including $\Lambda = 0$) that allow a recollapse (or the OSdS implosion from rest), $M < 1/3\Lambda^{1/2}$, the earliest null ray emitted from the portion of the past naked singularity not covered by dust (see Figs. 4 and 7) will reach the sphere’s center before the emergence of \mathcal{H}_h^+ (see the Appendix). This will allow an alert observer at $x = 0$ to avoid the future black-hole

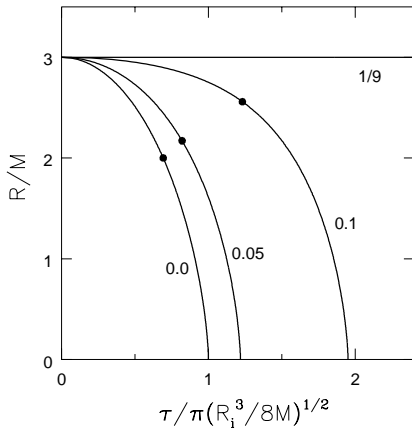


FIG. 5. OSdS collapse to a black hole. Shown is the evolution $R(\tau)$ of the surface of a dust sphere starting from rest at $R = 3M$ for the indicated values of ΛM^2 . The solid dots mark the points at which the spheres' surfaces cross their black-hole horizons.

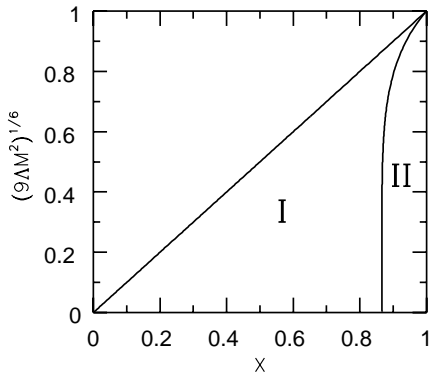


FIG. 6. Regions in the parameter space that allow an observer to escape from the recollapsing sphere to infinity after receiving at $x = 0$ the first signal from the dust-free portion of the past naked singularity (**I+II**) or from the past null infinity (**I**).

singularity if he heeds the warning coming from visible (assuming light can get through any finite-density region) sector of the initial singularity.

Instead of another sphere shown in Figs. 3 and 4, Fig. 7 is completed at the right by an infinite sequence of alternating Schwarzschild-de Sitter exteriors (with their characteristic cosmological horizons and spacelike null infinities) and black-hole interiors (bounded in the past and future by black-hole singularities).

For the special value $X = (9M^2\Lambda)^{1/6}$, the sphere can hover in a state of unstable equilibrium at the maximum of the effective potential at $R = r_m$. The Penrose diagram containing such a sphere is shown in Fig. 8.

Finally, for $M \leq 1/3\Lambda^{1/2}$ but $X < (9M^2\Lambda)^{1/6}$, a sphere contracting from $R = \infty$ at $\tau = -\infty$ will pass through \mathcal{H}_c^- and then form a black hole. Fig. 9 contains the corresponding Penrose diagram. Notice that at early

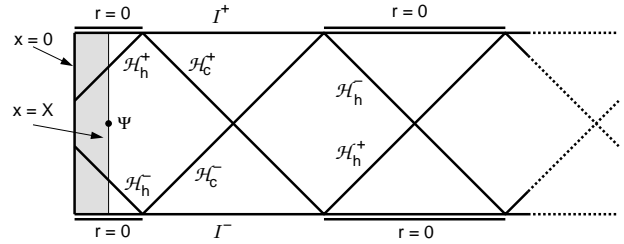


FIG. 7. A recollapsing sphere (compare Fig. 4) for parameters from region **I** of Fig. 6. Instead of another sphere to the right, the spacetime is closed off with an infinite series of alternating Schwarzschild-de Sitter exteriors and black-hole interiors.

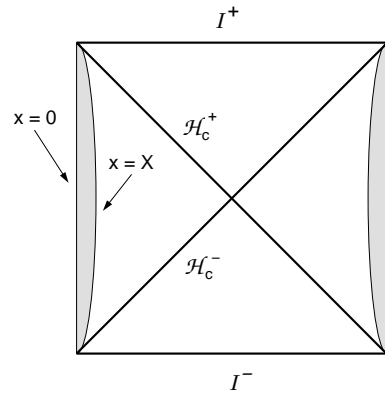


FIG. 8. A static dust sphere in unstable equilibrium for $X = (9M^2\Lambda)^{1/6}$.

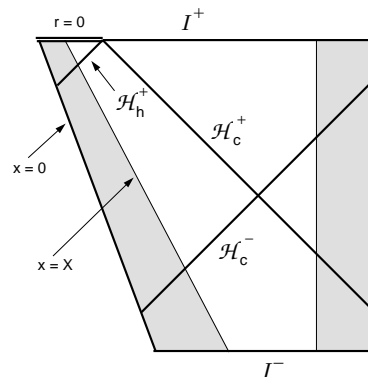


FIG. 9. Collapse into a black hole for $X < (9M^2\Lambda)^{1/6}$. The dust sphere's surface contracts through the past "cosmological horizon" \mathcal{H}_c^- , and then collapses to a black hole.

times the spacetime structure is similar to the early-time portion of the bouncing case (see Fig. 3), while the late-time evolution is akin to that of Fig. 4.

V. GLOBAL COLLAPSE

If $M > 1/3\Lambda^{1/2}$, $f(r)$ is negative everywhere and there is no static (i.e., with a time-like Killing vector) portion of the spacetime. The entire spacetime is analogous to the familiar vacuum Schwarzschild solution inside the event horizon, where the spacetime is dynamic and the radial and time coordinates reverse roles [see the last three paragraphs of Section 2]. Metric (2.15) describes a cylindrical spacelike hypersurface that shrinks (if the timelike coordinate $T \equiv -r$ is future directed) in the radial ($\dot{T} > 0$) direction and expands along its y -axis ($y \equiv t$) as the singularity at $T = 0$ is approached. At the left edge of this vacuum spacetime (see Fig. 10), the surface of the *collapsing* sphere recedes leftward along the y -axis, according to Eq. (2.16).

Since the integral $\int dy = -\int_{-\infty}^0 dT/g(T)$ is finite, a null ray travels only a finite difference Δy [see Eq. (2.17)] in the spacetime outside the sphere over the entire evolution from the past null infinity, $T = -\infty$, to the singularity at $T = 0$. This allows us to place another identical collapsing sphere (needed for geodesic completeness) receding to the right ($\dot{y} > 0$) of the first one (see Fig. 10) so that the two spheres either have causal contact (the specific case of Fig. 10) or are causally disconnected. In either case, the entire spacetime ends in a global cosmological singularity.

For $k = 0$ or $k = -1$, the static, momentarily static and bouncing solutions described above do not exist. Depending on whether $M < 1/3\Lambda^{1/2}$ [13] or not we have, respectively, a black hole formation shown in Fig. 9 or a “big crunch” shown in Fig. 10.

VI. SUMMARY

In this paper we have investigated the influence of a finite cosmological constant Λ on the evolution of a homogeneous sphere made of pressureless matter. In addition to Λ , the evolution is determined by the mass M of the sphere and the comoving extent, X , of the sphere interior’s spherical ($k = 1$), flat ($k = 0$) or hyperbolic ($k = -1$) slices of homogeneity.

A straightforward generalization of the familiar Oppenheimer-Snyder collapse from rest is possible only for $M < 1/3\Lambda^{1/2}$, $k = 1$ and $X > (9M^2\Lambda)^{1/6}$. In this case, the cosmological constant can slow down the collapse initially, but at later times the sphere’s self-gravity dominates entirely and eventually pulls the sphere into the final singularity.

The same range of parameters allows, however, a sphere contracting from large radii to avoid a collapse

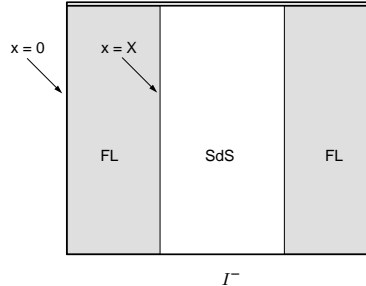


FIG. 10. Collapse into a global (cosmological) singularity for $M > 1/3\Lambda^{1/2}$.

and rebound en route to an exponential expansion at late times. In contrast to the previous case, the bouncing sphere’s evolution is dominated by the cosmological constant, with the matter playing the role of perturbation.

For all values of the parameters outside the above range, an initially contracting sphere will not be able to avoid being infinitely squeezed in the final singularity. The fate of the exterior spacetime depends, however, on the mass of the sphere: for $M < 1/3\Lambda^{1/2}$, the sphere forms its own black hole within its horizon, allowing the exterior space to expand exponentially at late times. For $M > 1/3\Lambda^{1/2}$, the sphere drags the entire spacetime into a “big crunch”: the exterior contracts on its way to the familiar de Sitter-like “throat” (see, e.g., [11]) but cannot escape out of it due to the overwhelming pull of the sphere’s gravity.

Acknowledgments

We wish to thank Dr. Thomas Baumgarte for stimulating discussions. This work was supported in part by NSF Grants AST 96-18524 and PHY 99-02833 and NASA Grants NAG 5-7152 and NAG 5-8418 at the University of Illinois at Urbana-Champaign.

APPENDIX A: EXTENSION OF THE COSMOLOGICAL AND BLACK HOLE HORIZONS INSIDE THE DUST SPHERE

1. Bouncing sphere

Solving Eq. (2.1) for future- and inward-directed radial null rays along \mathcal{H}_c^+ and integrating from the point ($R = r_c$) at which the re-expanding dust sphere’s surface crosses \mathcal{H}_c^+ (see Fig. 2), we obtain

$$\sin^{-1} X + \sin^{-1} x_f = \int_X^0 \frac{-dx}{\sqrt{1-x^2}} + \int_0^{x_f} \frac{dx}{\sqrt{1-x^2}}$$

$$\begin{aligned}
&= \Delta\zeta \equiv \int_{r_c/X}^{\infty} \frac{da}{a\dot{a}} \\
&= X \int_1^{\infty} \frac{dz}{\sqrt{z}} \frac{1}{(1-p+pz^3-X^2z)^{1/2}} \\
&\equiv F(X, p), \tag{A1}
\end{aligned}$$

where $p \equiv \Lambda r_c^2/3 = 1 - 2M/r_c$, $z \equiv R/r_c$ and x_f is the outermost point inside the dust sphere that can be reached by the null ray after it started at $x = X$ and then passed through the center $x = 0$. In Eq. (A1) we have introduced the conformal time $\zeta(\tau)$ of the FRW metric.

In the limit of vanishing mass, $p(M = 0) = 1$, $F(X, 1) = \sin^{-1} X$ and thus $x_f = 0$. This is the familiar structure of the de Sitter spacetime [12]. For $M > 0$, however, $x_f > 0$, and thus the center of the sphere, $x = 0$, will cross \mathcal{H}_c^+ at a finite proper time τ_c (as shown in Fig. 2).

This can be shown as follows. For any given Λ , $(\partial r_c/\partial M)_\Lambda = 2/(1-3p)$. Since p has the minimum value $p = 1/3$ for $M = 1/3\Lambda^{1/2}$ ($r_c = 3M = 1/\Lambda^{1/2}$, $f_{\max} = 0$), $(\partial r_c/\partial M)_\Lambda < 0$ and thus $(\partial p/\partial M)_\Lambda$ will always be negative. It then follows $(\partial F/\partial M)_X = (\partial F/\partial p)_X (\partial p/\partial M)_\Lambda > 0$. Hence, for any $M > 0$, $F[X, p(M)] > F[X, p(M = 0)] = \sin^{-1} X$ and thus $x_f > 0$. The surface $r = r_c$, therefore, loses for $M > 0$ the significance of an event horizon (with respect to the world line $x = 0$) that it has at $M = 0$.

2. Collapsing sphere

We now turn to the configuration of the past (\mathcal{H}_h^-) and the future (\mathcal{H}_h^+) black hole horizons. Measuring the conformal time of the FRW metric from the initial singularity

$$\begin{aligned}
\zeta(R) &\equiv \int_0^{R/X} \frac{da}{a\dot{a}} \\
&= 3\sqrt{3} \frac{X}{\sqrt{\lambda}} M \int_0^R \frac{dR}{|R(r_o - R)(r_b - R)(\bar{r}_3 - R)|^{1/2}}, \tag{A2}
\end{aligned}$$

where $\lambda \equiv 9\Lambda M^2$, and again solving Eq. (2.1) along the past black-hole event horizon, we find the value

$$\zeta_- = \zeta(r_h) + \sin^{-1} X, \tag{A3}$$

of the conformal time when the past black-hole horizon \mathcal{H}_h^- reaches the center of the sphere (see fig. 3). Notice that the conformal time depends only on X and ΛM^2 in addition to the current value of R .

Since the sphere's evolution is time-symmetric around the point of reversal r_o , the conformal time that elapses between the initial and past singularities is $2\zeta(r_o)$. Hence, the future black hole horizon \mathcal{H}_h^+ emerges from $x = 0$ at the conformal time

$$\zeta_+ = 2\zeta(r_o) - \zeta(r_h) - \sin^{-1} X. \tag{A4}$$

If the past horizon is to reach the sphere's center before the emergence of the future horizon, we must therefore have

$$\zeta(r_o) > \zeta(r_h) + \sin^{-1} X, \tag{A5}$$

the condition satisfied by all points in region **I** of the parameter space of Fig. 5 and by the specific case shown in the Penrose diagram of Fig. 6. If, on the other hand, we require that the null ray, emanating from the boundary between the sphere and the dust-free portion of the past singularity, gets at $\zeta = \sin^{-1} X$ to the sphere's center before the emergence of \mathcal{H}_h^+ , the following inequality needs to hold

$$\zeta(r_o) - \frac{1}{2}\zeta(r_h) > \sin^{-1} X. \tag{A6}$$

It turns out that condition (A6) is satisfied for all values of the parameters that allow a recollapse or an OSdS implosion.

In the case of a vanishing cosmological constant, $\zeta(r_o) - \zeta(r_h) = \pi - 2\sin^{-1} X$ and the condition (A5) is satisfied if $X < \sqrt{3}/2$. At the same time, $\zeta(r_o) - \frac{1}{2}\zeta(r_h) = \pi - \sin^{-1} X$, and the inequality (A6) holds if $X \leq 1$, which is satisfied by all recollapsing spheres.

-
- [1] A. G. Riess *et al.*, *Astron. J.* **116**, 1009 (1998).
 - [2] S. Perlmutter *et al.*, *Astrophys. J.* **517**, 565 (1999).
 - [3] I. Zehavi and A. Dekel, *Nature* **401**, 252 (1999).
 - [4] J. R. Oppenheimer and H. Snyder, *Phys. Rev.* **56**, 455 (1939).
 - [5] J. Morrow-Jones, PhD. Thesis, University of California, Santa Barbara (1988).
 - [6] F. Kottler, *Ann. Phys. (Leipzig)* **56**, 410 (1918).
 - [7] W. Israel, *Nuovo Cim.* **44B**, 1 (1966).
 - [8] Vacuum region **E** in Fig. 4.
 - [9] Vacuum regions **A** and **D** in Fig. 4.
 - [10] Vacuum regions **B** and **C** in Fig. 4.
 - [11] E. Schrödinger, *Expanding Universes*, Oxford University Press (1956).
 - [12] S. W. Hawking and G. F. R. Ellis, *The Large Scale Structure of Space-Time*, Cambridge University Press (1973).
 - [13] The critical mass satisfies $M_{crit} = 1/3\Lambda^{1/2} = 1.8 \times 10^{22} M_\odot (H_0/65 \text{ km/sec/Mpc})^{-1} \Omega_\Lambda^{-1/2}$, where recent Type Ia supernovae measurements give $\Omega_\Lambda = \Lambda/3H_0^2$ of order, but just below, unity [1,2]. Here H_0 is Hubble's constant.